

Separation of Reflection Components from a Color Image

Shoji Tominaga
Osaka Electro-Communication University
Neyagawa, Osaka 572, Japan

Abstract

A method is described for estimating the reflection components of glossy objects when the color signal is a mixture of body reflection, interface reflection, and interreflections. The objects are dielectric materials. We first model interreflection between two surfaces. Next, an algorithm is described for estimating the reflection components from a single color image. This estimation is performed in three steps of estimating illumination, object colors, and body interreflection. A chromaticity plane is introduced for analyzing the interreflection effects. We propose an algorithm for separating the measured image into the reflection components. The feasibility of the method is shown in experiments.

Introduction

The observed color vectors from an object surface of inhomogeneous dielectric materials are expressed in a linear combination of the body reflection and the interface reflection¹⁻³. When multiple objects of these materials are placed close, we observe mirror-like interreflections on the smooth surface from other nearby surfaces. By multiplication of dichromatic reflection, the interreflection between two surfaces is described as a sum of four terms including body-body reflection. This body interreflection was often neglected previously. This component was considered as being weak compared with the other components because (a) the reflected light was diffused widely and (b) the resulting reflectance was determined on multiplication of the body-spectral reflectances of both surfaces⁴. However it should be noted that the body interreflection is not decreased between similar object colors. This effect cannot be neglected.

The previous works on the reflection analysis are as follows: Klinker et al. introduced a dichromatic reflection model¹. Shafer et al. modeled reflection components under interreflection⁴. Funt et al. analyzed interreflection between two matte surfaces⁵. Bajcsy et al. detected highlights and interreflections by analyzing color histograms⁶. Tominaga described a method for estimating the surface-spectral reflectances of glossy objects from the spectral data⁷, where the body interreflection was not considered. No algorithm,

however, was given for estimating all color components of the complicated interreflections.

The present paper describes a method for estimating the four reflection components from a single color image of two closely apposed object surfaces. The objects are dielectric materials, and a color CCD camera is used for imaging under a single light source. The reflection components correspond to the illumination color, the two object colors, and the body interreflection color between two surfaces.

We first model interreflection between two surfaces. Next, an algorithm is described for estimating the reflection components from a single color image. This estimation is performed in three steps. The illumination is estimated from highlight areas in an image. We introduce a chromaticity plane for analyzing the chromaticity distribution of the image with interreflections. The object colors and the body interreflection are then estimated on the chromaticity distribution. Moreover, an algorithm is proposed for separating the measured image into the reflection components.

Modeling Reflection and Interreflection

Figure 1 shows interreflection between two nearby surfaces A and B. First, consider light reflection from a surface, A, by direct illumination from the single light source. This reflection consists of two terms of the body and interface reflection components. A nearby surface, B, provides a second source of illumination onto the surface A. Assume that the interreflection is based on only one bounce between two surfaces. The color signal from A is then described as

$$Y^A(x, \lambda) = w_b^A(x) S^A(\lambda) E(\lambda) + w_i^A(x) E(\lambda) + Y^{AB}(x, \lambda), \quad (1)$$

where $S^A(\lambda)$ is the body-spectral reflectance of A, and $w_b^A(x)$ and $w_i^A(x)$ are the weighting coefficients at location x on A. The first two terms in the right-hand side represent the dichromatic reflection by direct illumination. The third term $Y^{AB}(x, \lambda)$ represents the interreflection component by light reflected by the surface B.

This interreflection term is described as a sum of four terms of body-interface, interface-body, interface-interface, and body-body as shown in Figure 1. The term body-body represents the reflection process that body reflection occurs on both surfaces A and B. This interreflection is not neglected in this study. Grouping the reflection components yields a color signal containing four terms,

$$Y^A(x, \lambda) = w_{b2}^A(x) S^A(\lambda) E(\lambda) + w_{ib}^{AB}(x) S^B(\lambda) E(\lambda) + w_{i2}^A(x) E(\lambda) + w_{bb}^{AB}(x) S^A(\lambda) S^B(\lambda) E(\lambda) \quad (2)$$

The first term represents the object color of A. The second term is the object color of B by mirror-like reflection of A. The third term is the illumination color, which is produced by interface reflection of A and partly by interface-interface. The fourth term corresponds to the color produced by the body-body interreflection between A and B.

We can express the reflection model in terms of RGB values of a camera output. Define the four color vectors of object colors of A and B, illumination, and body interreflection as

$$\bar{\rho}^A = \begin{bmatrix} \rho_R^A \\ \rho_G^A \\ \rho_B^A \end{bmatrix}, \quad \bar{\rho}^B = \begin{bmatrix} \rho_R^B \\ \rho_G^B \\ \rho_B^B \end{bmatrix}, \quad \mathbf{e} = \begin{bmatrix} e_R \\ e_G \\ e_B \end{bmatrix}, \quad \bar{\rho}^{AB} = \begin{bmatrix} \rho_R^{AB} \\ \rho_G^{AB} \\ \rho_B^{AB} \end{bmatrix} \quad (3)$$

The observed vector $\bar{\rho}^A(x) = [\rho_R(x), \rho_G(x), \rho_B(x)]^t$ at pixel x on A is then described as follows:

$$\bar{\rho}^A(x) = w_{b2}^A(x) \bar{\rho}^A + w_{ib}^{AB}(x) \bar{\rho}^B + w_{i2}^A(x) \mathbf{e} + w_{bb}^{AB}(x) \bar{\rho}^{AB} \quad (4)$$

Thus the observations from A can be expressed in a linear combination of the four color components which are the two object colors of A and B, the light-source color, and the body interreflection color.

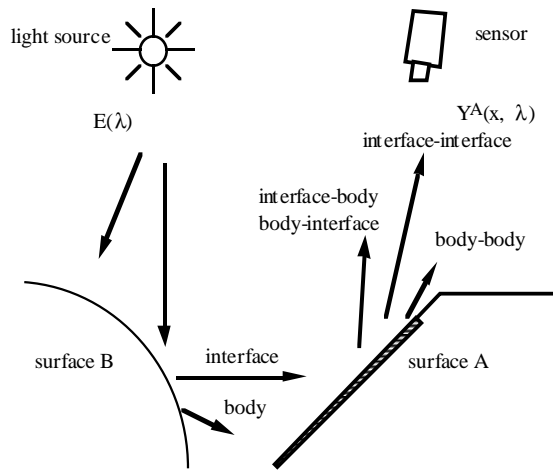


Figure 1 Observation of interreflection between two surfaces.

Estimation of Illumination Color

Because specular highlights include almost no interreflection effect, we can use highlight regions in the measured color image to estimate the illumination color \mathbf{e} . We have two approaches for the illumination estimation.

First, suppose that we have a single highlight region from a specular surface. We can use the pattern of color histogram to cluster the pixel data into interface and body reflection terms. The illuminant color is estimated from the directional vector of the interface cluster on the color

histogram. The algorithms are given by Klinker et al.⁷ and Tominaga⁸.

When we have more than two highlight regions from different objects, the illuminant estimation can be made even more reliably by using the algorithm by Tominaga and Wandell³. This algorithm takes advantage of the fact that each surface spans a two-dimensional color signal plane and that the intersection of the planes is a vector in the direction of the illumination color.

Estimating Reflection Components

Definition of chromaticity sphere and plane

To analyze the chromaticities of the observed colors, we define the chromaticity sphere. In this system the chromaticity coordinates for any observed color are specified on the basis of the chromaticity of illumination, which is different from the CIE xy-chromaticity plane. Figure 2 depicts this chromaticity sphere. All color vectors are normalized to a unit length, and mapped onto a unit sphere in a three-dimensional color space. Moreover we define the chromaticity plane. This plane is defined as a tangent plane that touches the chromaticity sphere at the illumination color vector as shown in Figure 2.

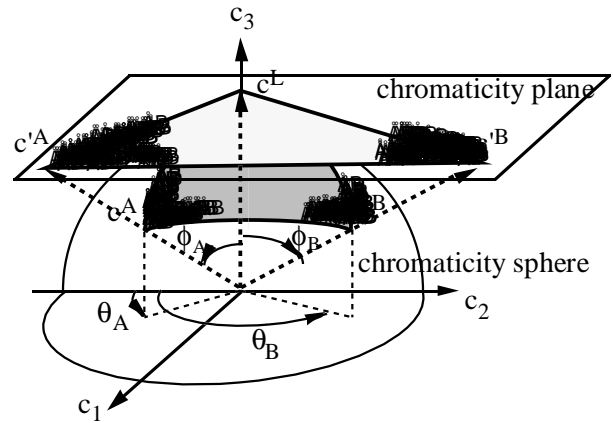


Figure 2 Chromaticity sphere and plane.

Chromaticity sphere:

In this system, the chromaticity of illumination is given as $\mathbf{c}^L = [0, 0, 1]^t$. This vector \mathbf{c}^L and the chromaticity vectors of two object colors \mathbf{c}^A and \mathbf{c}^B form a spherical triangle. The chromaticity of any observed color vector without interreflection effect is located theoretically in this spherical triangle. The polar coordinate system (ϕ, θ) is useful to represent the chromaticity in terms of hue and saturation, where the angle Θ corresponds to hue.

Chromaticity plane:

This plane is the tangent plane touching the chromaticity sphere at \mathbf{c}^L . A point on the chromaticity sphere is easily mapped onto the chromaticity plane. We extend a line connecting the origin and any coordinate point on the sphere. This extension line intersects the chromaticity plane. The coordinates (c_1', c_2') on the plane

can then be computed from the coordinates (c_1, c_2, c_3) on the sphere as

$$c_1' = c_1 / c_3, \quad c_2' = c_2 / c_3. \quad (5)$$

The illumination and two object colors form a triangle in this coordinate system. All the chromaticities observed from two surfaces fall in this triangle, unless the body interreflection occurs.

Estimation of object colors

The chromaticity vectors of object colors \mathbf{c}^A and \mathbf{c}^B are estimated from the chromaticity distribution of the measured image. Since these two vectors are two vertices of the triangle, the chromaticity estimation is reduced to determine the two vertices from the observed data on the chromaticity plane.

The coordinates of the vertices are determined in two steps. First we determine the hue angles θ^A and θ^B from peak analysis of the hue histogram. That is, we divide the whole angle of θ into a proper number of equal intervals to make the histogram, and find the segments corresponding to two peaks. Second, the farthest points from the origin \mathbf{c}^L are extracted from the data sets which belong to the same segments of θ . Let r_i be the distance between a chromaticity point from the origin. Then the estimates for \mathbf{c}^A and \mathbf{c}^B are represented in the polar coordinate system as

$$\mathbf{c}^A = (\max_i r_i, \theta^A), \quad \mathbf{c}^B = (\max_i r_i, \theta^B). \quad (6)$$

Estimation of body interreflection color

When the body interreflection occurs between two surfaces, the observed chromaticity coordinates do not always fall in the triangle on the chromaticity plane, but the distribution expands outside a triangle by \mathbf{c}^L , \mathbf{c}^A and \mathbf{c}^B as shown in Figure 3. Note that the two chromaticity clusters M_A and M_B located outside the segment $\overline{\mathbf{c}^A \mathbf{c}^B}$ represent the strong effect of the body interreflection. Image regions with this property correspond to the most close regions of two surfaces on the image. Hence we cut out two clusters of the body interreflection by the segment $\overline{\mathbf{c}^A \mathbf{c}^B}$, and extract the corresponding two image regions containing the body interreflection effect.

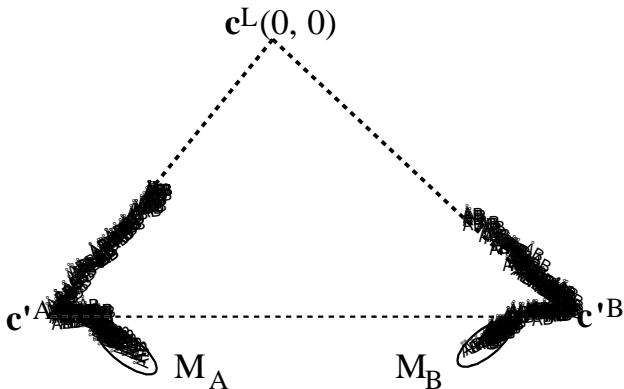


Figure 3 Chromaticity distribution of two surfaces containing body interreflection.

The RGB data in the extracted region are described as the linear combination of two color components $\bar{\rho}^A$ and $\bar{\rho}^{AB}$ for the surface A, and two color components $\bar{\rho}^B$ and $\bar{\rho}^{AB}$ for the surface B. The vectors $\bar{\rho}^A$ and $\bar{\rho}^B$ are already estimated in the above, and only $\bar{\rho}^{AB}$ is unknown as a common vector. Therefore the intersection algorithm³ is applicable for estimating $\bar{\rho}^{AB}$.

Image Decomposition

The measured image is decomposed into the reflection components by using the estimated color component vectors. For this decomposition, we have to determine the four weighting coefficients $w_{b2}^A(x)$, $w_{ib}^{AB}(x)$, $w_{i2}^A(x)$, and $w_{bb}^B(x)$ in Eq.(4) at each pixel. Note that the four unknown coefficients cannot be determined in the standard regression analysis because the image data are three-dimensional in a RGB space. In other words, we cannot determine four unknowns from only three observations.

We propose a solution method for this image separation problem by applying a linear programming technique. We use the constraints that all the unknown weighting coefficients must have non-negative values. Let us consider the estimation problem of the coefficients as the problem of minimizing the following absolute value of the residuals⁹:

$$|\bar{\rho}^A(x) - w_{b2}^A(x) \bar{\rho}^A - w_{ib}^{AB}(x) \bar{\rho}^B - w_{i2}^A(x) \mathbf{e} - w_{bb}^B(x) \bar{\rho}^{AB}| \rightarrow \min \quad (7)$$

First define several matrices and vectors. A matrix \mathbf{A} and a vector \mathbf{w} are defined as

$$\mathbf{A} = [a_{ij}] = [\mathbf{a}_1, \mathbf{a}_2, \mathbf{a}_3, \mathbf{a}_4] = [\bar{\rho}^A, \bar{\rho}^B, \mathbf{e}, \bar{\rho}^{AB}] \quad (8)$$

$$\mathbf{w} = [w_{b2}^A, w_{ib}^{AB}, w_{i2}^A, w_{bb}^B]^t. \quad (9)$$

For simplicity the observation vector is rewritten as

$$\mathbf{b} = \bar{\rho}(x). \quad (10)$$

The residual vector \mathbf{r} is then described as follows:

$$\mathbf{r} = [r_1, r_2, r_3]^t = \mathbf{b} - \mathbf{A} \mathbf{w}. \quad (11)$$

Note that r_i ($i=1, 2, 3$) is either positive, zero, or negative. When we split up r_i into two cases of non-negative and negative, we have either $r_i = r_i^+ \geq 0$ or $r_i = -r_i^- \leq 0$, i.e. $r_i = r_i^+ - r_i^-$ with $r_i^+ \times r_i^- = 0$. Thus the absolute values of the residual become $|r_i| = |r_i^+ - r_i^-| = r_i^+ + r_i^-$. Therefore the performance index of Eq.(7) can be written as

$$|\mathbf{r}| = (r_1^+ + r_1^-) + (r_2^+ + r_2^-) + (r_3^+ + r_3^-). \quad (12)$$

Moreover define a solution vector \mathbf{y} and a 3×10 augmented vector \mathbf{B} as

$$\mathbf{y} = [r_1^+, r_1^-, r_2^+, r_2^-, r_3^+, r_3^-, \mathbf{w}]^t \quad (13)$$

$$\mathbf{B} = [\mathbf{I}, -\mathbf{I}, \mathbf{A}]. \quad (14)$$

Then the constraint of Eq.(11) is written as $\mathbf{B} \mathbf{y} = \mathbf{b}$, where \mathbf{y} must be non-negative. Finally the above minimization problem can be reduced to the problem of solving the minimization of $|\mathbf{r}|$ under the constraints

$$\mathbf{B} \mathbf{y} = \mathbf{b}, \quad \mathbf{y} \geq 0. \quad (15)$$

This formulation becomes the standard form of a linear programming.

Experiments

Figure 4 shows the measured image of yellow (left) and green (right) plastic objects illuminated with a halogen lamp. Two highlight areas caused by direct specular reflection of illumination appeared in the sides of the two surfaces. Interreflection effects appeared closely to the contact line between the two surfaces. For illumination estimation, highlight regions with high values of luminance Y were extracted from the respective surfaces, and the illumination color was estimated by finding an intersection of color planes for two highlight regions.

The image region surrounded with a rectangle in Figure 4 was cut out to investigate the effects of interreflections in detail. The RGB data in this region were mapped onto the chromaticity plane. The chromaticities of the object colors were estimated based on the hue histogram analysis. Next, narrow regions close to the contact line between two surfaces were extracted as the regions with body interreflection. The color component of body interreflection was estimated from these two regions.

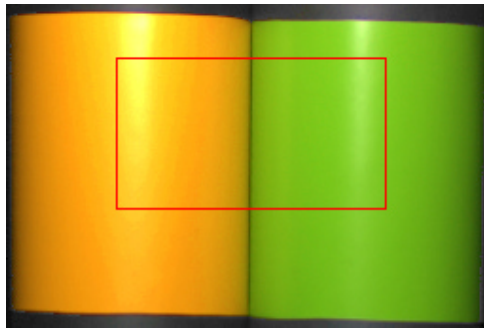
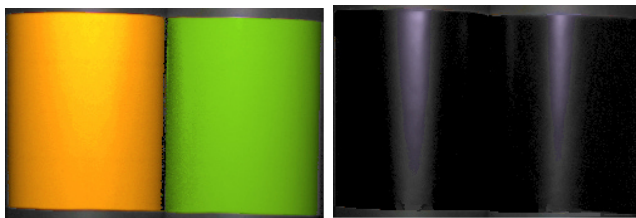
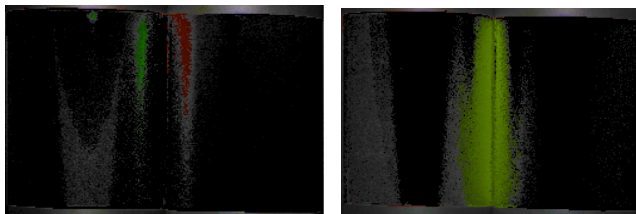


Figure 4 Image of two plastic objects.



(a) Object color component. (b) Illumination component.



(c) Specular interreflection. (d) Body interreflection.

Figure 5 Four Component images.

Finally the above separation algorithm was applied to all pixels of the measured image by using the estimated four color component vectors. Figure 5 shows the components of the image decomposed into the four reflection components.

Conclusion

The present paper has described a method for estimating the four reflection components from a single color image of two closely apposed object surfaces. The reflection components corresponded to the illumination color, the two object colors, and the body interreflection color between two surfaces. The objects were assumed to be inhomogeneous dielectric materials, and a color CCD camera was used for imaging under a single light source.

First, modeling interreflection between two object surfaces suggested that the observed color vectors from the surfaces were expressed in a linear combination of the four reflection components. Next, algorithms were described for estimating the reflection components from a single image. This estimation was performed in three steps of estimating the illumination, the object colors, and the body interreflection color. A chromaticity plane is useful for analyzing the chromaticity distribution of an image with the interreflection effects. Moreover, an algorithm was proposed for separating the measured image into the reflection components. The feasibility of the proposed method was demonstrated in experiments.

References

1. S.A.Shafer, Using color to separate reflection components, *Color Research and application*, **10**, 210-218, 1985.
2. G.J. Klinker, S.A. Shafer, and T. Kanade, The measurement of highlights in color images, *Int. J. Computer Vision*, **2**, 7-32, 1988.
3. S. Tominaga and B.A Wandell, The standard surface reflectance model and illuminant estimation, *J.Opt. Soc. Am. A*, **6**, 576-584, 1989.
4. S.A. Shafer, T. Kanade, G.J. Klinker, and C. L. Novak, Physics-based models for early vision by machine, *SPIE Proceedings*, **1250**, 222-235, 1990.
5. B.V. Funt and M.S. Drew, Color space analysis of mutual illumination, *IEEE Trans. on PAMI*, **15**, 1319-1326, 1993.
6. R.Bajcsy, S.W.Lee, and A.Leonards, Detection of diffuse and specular interface reflections and inter-reflections by color image segmentation, *Int. J. Computer Vision*, **17**, 241-272, 1996.
7. S. Tominaga, Surface reflectance estimation by the dichromatic model, *Color Research and application*, **21**, 104-114, 1996.
8. G.J. Klinker, S.A. Shafer, and T. Kanade, A physical approach to color image understanding, *Int. J. Computer Vision*, **4**, 7-38, 1990.
9. H.Spath, *Mathematical Algorithms for Linear Regression*, p. 58, Academic Press, 1992.